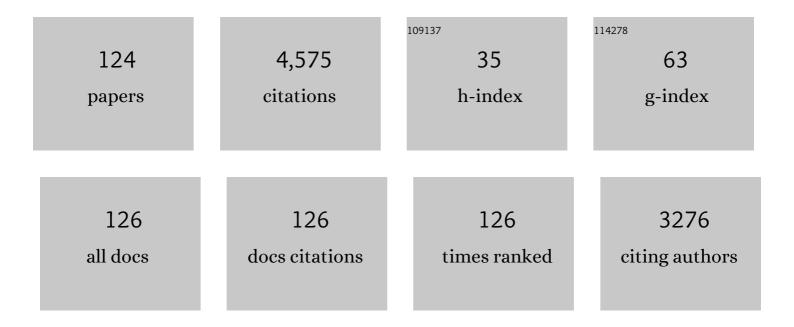
List of Publications by Year in descending order

Source: https://exaly.com/author-pdf/7346552/publications.pdf Version: 2024-02-01



ΥλΝΗΤΝ ΓΙ

#	Article	IF	CITATIONS
1	Dislocation behavior in a polycrystalline Mg-Y alloy using multi-scale characterization and VPSC simulation. Journal of Materials Science and Technology, 2022, 98, 87-98.	5.6	36
2	Sn-Aided Joining of Cast Aluminum and Steel Through a Compound Casting Process. Metallurgical and Materials Transactions B: Process Metallurgy and Materials Processing Science, 2022, 53, 60-70.	1.0	7
3	Synergistic effects of Cd, Si and Cr additions on precipitation strengthening and thermal stability of dispersoids in AA3003 alloy. Materials Science & Engineering A: Structural Materials: Properties, Microstructure and Processing, 2022, 832, 142422.	2.6	5
4	Effect of Inclusion and Filtration on Grain Refinement Efficiency of Aluminum Alloy. Metallurgical and Materials Transactions A: Physical Metallurgy and Materials Science, 2022, 53, 1000-1012.	1.1	1
5	The role of grain boundary plane in slip transfer during deformation of magnesium alloys. Acta Materialia, 2022, 227, 117662.	3.8	25
6	Freezing solute atoms in nanograined aluminum alloys via high-density vacancies. Nature Communications, 2022, 13, .	5.8	18
7	Growth kinetics of primary Si particles in hypereutectic Al-Si alloys under the influence of P inoculation: Experiments and modelling. Journal of Alloys and Compounds, 2021, 854, 155323.	2.8	15
8	Interfacial Microstructure Formation in Al7SiMg/Cu Compound Castings. International Journal of Metalcasting, 2021, 15, 40-48.	1,5	15
9	Facile fabrication of ultrathin freestanding nanoporous Cu and Cu-Ag films with high SERS sensitivity by dealloying Mg-Cu(Ag)-Gd metallic glasses. Journal of Materials Science and Technology, 2021, 70, 205-213.	5.6	11
10	Influence of Grain Refiners on the Wettability of Al2O3 Substrate by Aluminum Melt. Metallurgical and Materials Transactions B: Process Metallurgy and Materials Processing Science, 2021, 52, 382-392.	1.0	13
11	The Effect of Grain Refiner on Aluminium Filtration. Minerals, Metals and Materials Series, 2021, , 803-809.	0.3	0
12	Achieving high-strength metallurgical bonding between A356 aluminum and copper through compound casting. Materials Science & Engineering A: Structural Materials: Properties, Microstructure and Processing, 2021, 810, 140979.	2.6	12
13	The Interactions Between Oxide Film Inclusions and Inoculation Particles TiB2 in Aluminum Melt. Metallurgical and Materials Transactions B: Process Metallurgy and Materials Processing Science, 2021, 52, 2497-2508.	1.0	9
14	Synergistic strengthening by nano-sized α-Al(Mn,Fe)Si and Al3Zr dispersoids in a heat-resistant Al–Mn–Fe–Si–Zr alloy. Materials Science & Engineering A: Structural Materials: Properties, Microstructure and Processing, 2021, 819, 141460.	2.6	20
15	Facile synthesis of metal and alloy nanoparticles by ultrasound-assisted dealloying of metallic glasses. Journal of Materials Science and Technology, 2021, 82, 144-152.	5.6	8
16	The Influences of Grain Refiner, Inclusion Level, and Filter Grade on the Filtration Performance of Aluminum Melt. Metallurgical and Materials Transactions B: Process Metallurgy and Materials Processing Science, 2021, 52, 3946-3960.	1.0	3
17	Microstructures and mechanical properties of nano-C and in situ Al2O3 reinforced aluminium matrix composites processed by equal-channel angular pressing. Journal of Alloys and Compounds, 2021, 876, 160159.	2.8	13
18	Prominent role of multi-scale microstructural heterogeneities on superplastic deformation of a high solid solution Al–7Mg alloy. International Journal of Plasticity, 2021, 146, 103108.	4.1	38

#	Article	IF	CITATIONS
19	Nanoparticle additions promote outstanding fracture toughness and fatigue strength in a cast Al–Cu alloy. Materials and Design, 2020, 186, 108221.	3.3	17
20	Modelling the Age-Hardening Precipitation by a Revised Langer and Schwartz Approach with Log-Normal Size Distribution. Metallurgical and Materials Transactions A: Physical Metallurgy and Materials Science, 2020, 51, 4838-4852.	1.1	14
21	Microstructural considerations of enhanced tensile strength and mechanical constraint in a copper/stainless steel brazed joint. Materials Science & Engineering A: Structural Materials: Properties, Microstructure and Processing, 2020, 796, 139992.	2.6	11
22	Revealing the Subsurface Basal 〈a〉 Dislocation Activity in Magnesium Through Lattice Rotation Analysis. Metallurgical and Materials Transactions A: Physical Metallurgy and Materials Science, 2020, 51, 4414-4421.	1.1	7
23	Revealing the nucleation kinetics of primary Si particles in hypereutectic Al–Si alloys under the influence of P inoculation. Journal of Materials Science, 2020, 55, 15621-15635.	1.7	17
24	Formation and evolution of the interfacial structure in al/steel compound castings during solidification and heat treatment. Journal of Alloys and Compounds, 2020, 849, 156685.	2.8	28
25	Enhanced nucleation and precipitation hardening in Al–Mg–Si(–Cu) alloys with minor Cd additions. Materials Science & Engineering A: Structural Materials: Properties, Microstructure and Processing, 2020, 792, 139698.	2.6	18
26	Revealing slip-induced extension twinning behaviors dominated by micro deformation in a magnesium alloy. International Journal of Plasticity, 2020, 128, 102669.	4.1	41
27	In-situ X-radiographic study of nucleation and growth behaviour of primary silicon particles during solidification of a hypereutectic Al-Si alloy. Journal of Alloys and Compounds, 2020, 832, 154948.	2.8	13
28	Texture evolution of an Al-8Zn alloy during ECAP and post-ECAP isothermal annealing. Materials Characterization, 2019, 155, 109794.	1.9	10
29	Accelerated recrystallization by electric current flash heating in cold-rolled Al-5Cu alloy under the influence of concurrent precipitation. Journal of Alloys and Compounds, 2019, 811, 151891.	2.8	4
30	Effect of Ag addition on the precipitation evolution and interfacial segregation for Al–Mg–Si alloy. Acta Materialia, 2019, 180, 301-316.	3.8	76
31	Precipitation in an A356 foundry alloy with Cu additions - A transmission electron microscopy study. Journal of Alloys and Compounds, 2019, 785, 1106-1114.	2.8	31
32	Influence of Cu addition on the heat treatment response of A356 foundry alloy. Materials Today Communications, 2019, 19, 342-348.	0.9	17
33	Revealing the Heterogeneous Nucleation and Growth Behaviour of Grains in Inoculated Aluminium Alloys During Solidification. Minerals, Metals and Materials Series, 2019, , 1665-1675.	0.3	0
34	AlSi10Mg alloy nanocomposites reinforced with aluminum-coated graphene: Selective laser melting, interfacial microstructure and property analysis. Journal of Alloys and Compounds, 2019, 792, 203-214.	2.8	147
35	Revealing the factors influencing grain boundary segregation of P, As in Si: Insights from first-principles. Acta Materialia, 2019, 168, 52-62.	3.8	26
36	Study of Controllable Inclusion Addition Methods in Al Melt. Minerals, Metals and Materials Series, 2019, , 1041-1048.	0.3	2

#	Article	IF	CITATIONS
37	β- and δ-Al-Fe-Si intermetallic phase, their intergrowth and polytype formation. Journal of Alloys and Compounds, 2019, 780, 917-929.	2.8	27
38	Revealing abnormal {11 <mml:math <br="" altimg="si1.gif" xmlns:mml="http://www.w3.org/1998/Math/MathML">overflow="scroll"><mml:mrow><mml:mover accent="true"><mml:mrow><mml:mn>2</mml:mn></mml:mrow><mml:mo stretchy="true">Â⁻</mml:mo </mml:mover </mml:mrow></mml:math> 1} twins in commercial purity Ti subjected to split Hopkinson pressure bar. Journal of Alloys and Compounds, 2019, 783, 513-523.	2.8	5
39	Effect of Mn and cooling rates on α-, β- and δ-Al–Fe–Si intermetallic phase formation in a secondary Al–Si alloy. Materialia, 2019, 5, 100198.	1.3	57
40	Revealing the heterogeneous nucleation behavior of equiaxed grains of inoculated Al alloys during directional solidification. Acta Materialia, 2018, 149, 312-325.	3.8	87
41	Segregation of Mg, Cu and their effects on the strength of Al Σ5 (210)[001] symmetrical tilt grain boundary. Acta Materialia, 2018, 145, 235-246.	3.8	101
42	A Thermodynamic Study on the Effect of Solute on the Nucleation Driving Force, Solid–Liquid Interfacial Energy, and Grain Refinement of Al Alloys. Metallurgical and Materials Transactions A: Physical Metallurgy and Materials Science, 2018, 49, 1770-1781.	1.1	19
43	Carbon segregation at Σ3 {1â€~1â€~2} grain boundaries in silicon. Computational Materials Science, 2018, 143, 80-86.	1.4	13
44	Modelling microstructure evolution during casting, homogenization and ageing heat treatment of Al-Mg-Si-Cu-Fe-Mn alloys. Calphad: Computer Coupling of Phase Diagrams and Thermochemistry, 2018, 63, 164-184.	0.7	21
45	Grain Boundary Segregation in Pd-Cu-Ag Alloys for High Permeability Hydrogen Separation Membranes. Membranes, 2018, 8, 81.	1.4	7
46	Improving ageing kinetics and precipitation hardening in an Al-Mg-Si alloy by minor Cd addition. Materialia, 2018, 4, 33-37.	1.3	15
47	Formation of Σ3{110} incoherent twin boundaries through geometrically necessary boundaries in an Al-8Zn alloy subjected to one pass of equal channel angular pressing. Journal of Alloys and Compounds, 2018, 762, 190-195.	2.8	12
48	Enhanced dispersoid precipitation and dispersion strengthening in an Al alloy by microalloying with Cd. Acta Materialia, 2018, 157, 114-125.	3.8	79
49	Quantifying the grain boundary segregation strengthening induced by post-ECAP aging in an Al-5Cu alloy. Acta Materialia, 2018, 155, 199-213.	3.8	62
50	Lattice distortion induced site dependent carbon gettering at twin boundaries in silicon. Journal of Alloys and Compounds, 2017, 712, 599-604.	2.8	21
51	The deformation and work hardening behaviour of a SPD processed Al-5Cu alloy. Journal of Alloys and Compounds, 2017, 697, 239-248.	2.8	28
52	Effect of soft Bi particles on grain refinement during severe plastic deformation. Transactions of Nonferrous Metals Society of China, 2017, 27, 971-976.	1.7	7
53	Heterogeneous nucleation and grain growth of inoculated aluminium alloys: An integrated study by in-situ X-radiography and numerical modelling. Acta Materialia, 2017, 140, 224-239.	3.8	102
54	Soft particles assisted grain refinement and strengthening of an Al-Bi-Zn alloy subjected to ECAP. Materials Science & Engineering A: Structural Materials: Properties, Microstructure and Processing, 2017, 703, 304-313.	2.6	15

#	Article	IF	CITATIONS
55	Twinnability of Al–Mg alloys: A first-principles interpretation. Transactions of Nonferrous Metals Society of China, 2017, 27, 1313-1318.	1.7	3
56	Combined effect of Mg and vacancy on the generalized planar fault energy of Al. Journal of Alloys and Compounds, 2017, 690, 841-850.	2.8	21
57	Morphological Transition of α-Mg Dendrites During Near-Isothermal Solidification of a Mg–Nd〓Gd–Zn–Zr Casting Alloy. Minerals, Metals and Materials Series, 2017, , 591-596.	0.3	0
58	The Influence of Processing Conditions on Microchemistry and the Softening Behavior of Cold Rolled Al-Mn-Fe-Si Alloys. Metals, 2016, 6, 61.	1.0	7
59	Roles of Alloy Composition and Grain Refinement on Hot Tearing Susceptibility of 7××× Aluminum Alloys. Metallurgical and Materials Transactions A: Physical Metallurgy and Materials Science, 2016, 47, 4080-4091.	1.1	30
60	The orientation relationships of nanobelt-like Si ₂ Hf precipitates in an Al–Si–Mg–Hf alloy. Journal of Applied Crystallography, 2016, 49, 1223-1230.	1.9	7
61	Impurity effect of Mg on the generalized planar fault energy of Al. Journal of Materials Science, 2016, 51, 6552-6568.	1.7	46
62	Formation of <mml:math <br="" altimg="si1.gif" xmlns:mml="http://www.w3.org/1998/Math/MathML">overflow="scroll"><mml:mrow><mml:mrow><mml:mo>{</mml:mo><mml:mrow><mml:mrow><mml:mrow><mml:mrow><mml:mrow><mml:mrow><mml:mrow><mml:mrow><mml:mrow><mml:mrow><mml:mrow><mml:mrow><mml:mrow><mml:mrow><mml:mrow><mml:mrow><mml:mrow><mml:mrow><mml:mrow><mml:mrow><mml:mrow><mml:mrow><mml:mrow><mml:mrow><mml:mrow><mml:mrow><mml:mrow><mml:mrow><mml:mrow><mml:mrow><mml:mrow><mml:mrow><mml:mrow><mml:mrow><mml:mrow><mml:mrow><mml:mrow><mml:mrow><mml:mrow><mml:mrow><mml:mrow><mml:mrow><mml:mrow><mml:mrow><mml:mrow><mml:mrow><mml:mrow><mml:mrow><mml:mrow><mml:mrow><mml:mrow><mml:mrow><mml:mrow><mml:mrow><mml:mrow><mml:mrow><mml:mrow><mml:mrow><mml:mrow><mml:mrow><mml:mrow><mml:mrow><mml:mrow><mml:mrow><mml:mrow><mml:mrow><mml:mrow><mml:mrow><mml:mrow><mml:mrow><mml:mrow><mml:mrow><mml:mrow><mml:mrow><mml:mrow><mml:mrow><mml:mrow><mml:mrow><mml:mrow><mml:mrow><mml:mrow><mml:mrow><mml:mrow><mml:mrow><mml:mrow><mml:mrow><mml:mrow><mml:mrow><mml:mrow><mml:mrow><mml:mrow><mml:mrow><mml:mrow><mml:mrow><mml:mrow><mml:mrow><mml:mrow><mml:mrow><mml:mrow><mml:mrow><mml:mrow><mml:mrow><mml:mrow><mml:mrow><mml:mrow><mml:mrow><mml:mrow><mml:mrow><mml:mrow><mml:mrow><mml:mrow><mml:mrow><mml:mrow><mml:mrow><mml:mrow><mml:mrow><mml:mrow><mml:mrow><mml:mrow><mml:mrow><mml:mrow><mml:mrow><mml:mrow><mml:mrow><mml:mrow><mml:mrow><mml:mrow><mml:mrow><mml:mrow><mml:mrow><mml:mrow><mml:mrow><mml:mrow><mml:mrow><mml:mrow><mml:mrow><mml:mrow><mml:mrow><mml:mrow><mml:mrow><mml:mrow><mml:mrow><mml:mrow><mml:mrow><mml:mrow><mml:mrow><mml:mrow><mml:mrow><mml:mrow><mml:mrow><mml:mrow><mml:mrow><mml:mrow><mml:mrow><mml:mrow><mml:mrow><mml:mrow><mml:mrow><mml:mrow><mml:mrow><mml:mrow><mml:mrow><mml:mrow><mml:mrow><mml:mrow><mml:mrow><mml:mrow><mml:mrow><mml:mrow><mml:mrow><mml:mrow><mml:mrow><mml:mrow><mml:mrow><mml:mrow><mml:mrow><mml:mrow><mml:mrow><mml:mrow><mml:mrow><mml:mrow><mml:mrow><mml:mrow><mml:mrow><mml:mrow><mml:mrow><mml:mrow><mml:mrow><mml:mrow><mml:mrow><mm< td=""><td>mrow><m າສເ\$mml:n</m </td><td>ml:mover næw><mml< td=""></mml<></td></mm<></mml:mrow></mml:mrow></mml:mrow></mml:mrow></mml:mrow></mml:mrow></mml:mrow></mml:mrow></mml:mrow></mml:mrow></mml:mrow></mml:mrow></mml:mrow></mml:mrow></mml:mrow></mml:mrow></mml:mrow></mml:mrow></mml:mrow></mml:mrow></mml:mrow></mml:mrow></mml:mrow></mml:mrow></mml:mrow></mml:mrow></mml:mrow></mml:mrow></mml:mrow></mml:mrow></mml:mrow></mml:mrow></mml:mrow></mml:mrow></mml:mrow></mml:mrow></mml:mrow></mml:mrow></mml:mrow></mml:mrow></mml:mrow></mml:mrow></mml:mrow></mml:mrow></mml:mrow></mml:mrow></mml:mrow></mml:mrow></mml:mrow></mml:mrow></mml:mrow></mml:mrow></mml:mrow></mml:mrow></mml:mrow></mml:mrow></mml:mrow></mml:mrow></mml:mrow></mml:mrow></mml:mrow></mml:mrow></mml:mrow></mml:mrow></mml:mrow></mml:mrow></mml:mrow></mml:mrow></mml:mrow></mml:mrow></mml:mrow></mml:mrow></mml:mrow></mml:mrow></mml:mrow></mml:mrow></mml:mrow></mml:mrow></mml:mrow></mml:mrow></mml:mrow></mml:mrow></mml:mrow></mml:mrow></mml:mrow></mml:mrow></mml:mrow></mml:mrow></mml:mrow></mml:mrow></mml:mrow></mml:mrow></mml:mrow></mml:mrow></mml:mrow></mml:mrow></mml:mrow></mml:mrow></mml:mrow></mml:mrow></mml:mrow></mml:mrow></mml:mrow></mml:mrow></mml:mrow></mml:mrow></mml:mrow></mml:mrow></mml:mrow></mml:mrow></mml:mrow></mml:mrow></mml:mrow></mml:mrow></mml:mrow></mml:mrow></mml:mrow></mml:mrow></mml:mrow></mml:mrow></mml:mrow></mml:mrow></mml:mrow></mml:mrow></mml:mrow></mml:mrow></mml:mrow></mml:mrow></mml:mrow></mml:mrow></mml:mrow></mml:mrow></mml:mrow></mml:mrow></mml:mrow></mml:mrow></mml:mrow></mml:mrow></mml:mrow></mml:mrow></mml:mrow></mml:mrow></mml:mrow></mml:mrow></mml:mrow></mml:mrow></mml:mrow></mml:mrow></mml:mrow></mml:mrow></mml:mrow></mml:mrow></mml:mrow></mml:mrow></mml:mrow></mml:mrow></mml:mrow></mml:mrow></mml:mrow></mml:mrow></mml:mrow></mml:mrow></mml:mrow></mml:mrow></mml:mrow></mml:mrow></mml:mrow></mml:mrow></mml:mrow></mml:mrow></mml:mrow></mml:mrow></mml:mrow></mml:mrow></mml:mrow></mml:mrow></mml:mrow></mml:mrow></mml:mrow></mml:mrow></mml:mrow></mml:mrow></mml:mrow></mml:mrow></mml:mrow></mml:mrow></mml:mrow></mml:mrow></mml:mrow></mml:mrow></mml:mrow></mml:mrow></mml:math>	mrow> <m າສເ\$mml:n</m 	ml:mover næw> <mml< td=""></mml<>
63	α-Mg primary phase formation and dendritic morphology transition in solidification of a Mg-Nd-Gd-Zn-Zr casting alloy. Acta Materialia, 2016, 116, 177-187.	3.8	36
64	Aluminium substituted lanthanum based perovskite type oxides, non-stoichiometry and performance in methane partial oxidation by framework oxygen. Applied Catalysis A: General, 2016, 523, 171-181.	2.2	11
65	Orientation Preference of Recrystallization in Supersaturated Aluminum Alloys Influenced by Concurrent Precipitation. Metallurgical and Materials Transactions A: Physical Metallurgy and Materials Science, 2016, 47, 1378-1388.	1.1	22
66	Precipitation of Dispersoids in DC-Cast AA3103 Alloy during Heat Treatment. , 2016, , 1021-1027.		6
67	Growth Directions of Precipitates in the Al–Si–Mg–Hf Alloy Using Combined EBSD and FIB 3D-Reconstruction Techniques. Microscopy and Microanalysis, 2015, 21, 588-593.	0.2	8
68	Formation of incoherent deformation twin boundaries in a coarse-grained Al-7Mg alloy. Applied Physics Letters, 2015, 107, 091901.	1.5	15
69	Numerical modelling and in-situ radiographic study of the grain nucleation and growth of inoculated aluminum alloys. IOP Conference Series: Materials Science and Engineering, 2015, 84, 012090.	0.3	3
70	Prediction of as-cast grain size of inoculated aluminum alloys melt solidified under non-isothermal conditions. IOP Conference Series: Materials Science and Engineering, 2015, 84, 012015.	0.3	4
71	Factors affecting the strength of P{011}〈566〉-texture after annealing of a cold-rolled Al–Mn–Fe–Si alloy. Journal of Materials Science, 2015, 50, 5091-5103.	1.7	17
72	Deformation of an Al–7Mg alloy with extensive structural micro-segregations during dynamic plastic deformation. Materials Science & Engineering A: Structural Materials: Properties, Microstructure and Processing, 2015, 628, 160-167.	2.6	26

#	Article	IF	CITATIONS
73	Evolution in microstructure and properties during non-isothermal annealing of a cold-rolled Al–Mn–Fe–Si alloy with different microchemistry states. Materials Science & Engineering A: Structural Materials: Properties, Microstructure and Processing, 2015, 628, 216-229.	2.6	41
74	Two-stage annealing of a cold-rolled Al–Mn–Fe–Si alloy with different microchemistry states. Journal of Materials Processing Technology, 2015, 221, 87-99.	3.1	39
75	Effect of heterogeneously distributed pre-existing dispersoids on the recrystallization behavior of a cold-rolled Al–Mn–Fe–Si alloy. Materials Characterization, 2015, 102, 92-97.	1.9	45
76	High ductility bulk nanostructured Al–Mg binary alloy processed by equal channel angular pressing and inter-pass annealing. Scripta Materialia, 2015, 105, 22-25.	2.6	47
77	The influence of microchemistry on the recrystallization texture of cold-rolled Al-Mn-Fe-Si alloys. IOP Conference Series: Materials Science and Engineering, 2015, 82, 012035.	0.3	2
78	Combining HAADF STEM tomography and electron diffraction for studies of α-Al(Fe,Mn)Si dispersoids in 3xxx aluminium alloys. Philosophical Magazine, 2015, 95, 744-758.	0.7	12
79	Influence of Dendritic Growth of Equiaxed Grains on As-Cast Grain Size Prediction of Inoculated Aluminum Alloys. Transactions of the Indian Institute of Metals, 2015, 68, 1013-1016.	0.7	3
80	Multi-component solid solution and cluster hardening of Al–Mn–Si alloys. Materials Science & Engineering A: Structural Materials: Properties, Microstructure and Processing, 2015, 625, 153-157.	2.6	19
81	Microstructure evolution and mechanical behavior of a binary Al–7Mg alloy processed by equal-channel angular pressing. Acta Materialia, 2015, 84, 42-54.	3.8	220
82	Isothermal annealing of cold-rolled Al–Mn–Fe–Si alloy with different microchemistry states. Transactions of Nonferrous Metals Society of China, 2014, 24, 3840-3847.	1.7	12
83	Prediction of solute diffusivity in Al assisted by first-principles molecular dynamics. Journal of Physics Condensed Matter, 2014, 26, 025403.	0.7	5
84	An extension of the Kampmann–Wagner numerical model towards as-cast grain size prediction of multicomponent aluminum alloys. Acta Materialia, 2014, 71, 380-389.	3.8	84
85	Dispersion of soft Bi particles and grain refinement of matrix in an Al–Bi alloy by equal channel angular pressing. Journal of Alloys and Compounds, 2014, 605, 131-136.	2.8	26
86	Novel deformation structures of pure titanium induced by room temperature equal channel angular pressing. Materials Letters, 2014, 117, 195-198.	1.3	21
87	Effect modeling of Cr and Zn on microstructure evolution during homogenization heat treatment of AA3xxx alloys. Transactions of Nonferrous Metals Society of China, 2014, 24, 2145-2149.	1.7	12
88	Morphology and size control of octahedral and cubic primary Mg ₂ Si in an Mg–Si system by regulating Sr contents. CrystEngComm, 2014, 16, 448-454.	1.3	46
89	Retrieval of three-dimensional spatial information from fast in situ two-dimensional synchrotron radiography of solidification microstructure evolution. Acta Materialia, 2014, 81, 241-247.	3.8	49
90	Mackay icosahedron explaining orientation relationship of dispersoids in aluminium alloys. Acta Crystallographica Section B: Structural Science, Crystal Engineering and Materials, 2014, 70, 888-896.	0.5	7

#	Article	IF	CITATIONS
91	Microstructure, hardness evolution and thermal stability of binary Al-7Mg alloy processed by ECAP with intermediate annealing. Transactions of Nonferrous Metals Society of China, 2014, 24, 2301-2306.	1.7	26
92	Composition and orientation relationships of constituent particles in 3xxx aluminum alloys. Philosophical Magazine, 2014, 94, 556-568.	0.7	24
93	Grain boundary segregation engineering in metallic alloys: A pathway to the design of interfaces. Current Opinion in Solid State and Materials Science, 2014, 18, 253-261.	5.6	466
94	The influence of microchemistry on the softening behaviour of two cold-rolled Al–Mn–Fe–Si alloys. Materials Science & Engineering A: Structural Materials: Properties, Microstructure and Processing, 2014, 601, 86-96.	2.6	47
95	Achieve high ductility and strength in an Al–Mg alloy by severe plastic deformation combined with inter-pass annealing. Materials Science & Engineering A: Structural Materials: Properties, Microstructure and Processing, 2014, 598, 141-146.	2.6	60
96	Prediction of elastic properties of nanofibrillated cellulose from micromechanical modeling and nano-structure characterization by transmission electron microscopy. Cellulose, 2013, 20, 761-770.	2.4	25
97	Dispersoid strengthening in AA3xxx alloys with varying Mn and Si content during annealing at low temperatures. Materials Science & Engineering A: Structural Materials: Properties, Microstructure and Processing, 2013, 567, 21-28.	2.6	111
98	Annealing response of binary Al–7Mg alloy deformed by equal channel angular pressing. Materials Science & Engineering A: Structural Materials: Properties, Microstructure and Processing, 2013, 586, 374-381.	2.6	28
99	Effect of stoichiometry on the surface energies of {100} and {111} and the crystal shape of TiCx and TiNx. CrystEngComm, 2013, 15, 643-649.	1.3	39
100	Characterization the Softening Behavior of Cold Rolled AlMnFeSi-Alloys during Conditions of Concurrent Precipitation. Materials Science Forum, 2013, 753, 231-234.	0.3	4
101	Influence of dispersoids on microstructure evolution and work hardening of aluminium alloys during tension and cold rolling. Philosophical Magazine, 2013, 93, 2995-3011.	0.7	35
102	Synthesis of spherical NbB2â^'x particles by controlling the stoichiometry. CrystEngComm, 2012, 14, 1925.	1.3	14
103	Effects of La on the age hardening behavior and precipitation kinetics in the cast Al–Cu alloy. Journal of Alloys and Compounds, 2012, 540, 154-158.	2.8	26
104	Evolution in microstructure and mechanical properties during back-annealing of AlMnFeSi alloy. Transactions of Nonferrous Metals Society of China, 2012, 22, 1878-1883.	1.7	9
105	Precipitation crystallography of plate-shaped Al6(Mn,Fe) dispersoids in AA5182 alloy. Acta Materialia, 2012, 60, 5963-5974.	3.8	83
106	Microstructural heterogeneity in hexagonal close-packed pure Ti processed by high-pressure torsion. Journal of Materials Science, 2012, 47, 4838-4844.	1.7	18
107	Precipitation of partially coherent α-Al(Mn,Fe)Si dispersoids and their strengthening effect in AA 3003 alloy. Acta Materialia, 2012, 60, 1004-1014.	3.8	197
108	Through-process sensitivity analysis on the effect of process variables on strength in extruded Al–Mg–Si alloys. Journal of Materials Processing Technology, 2012, 212, 171-180.	3.1	10

#	Article	IF	CITATIONS
109	Orientation Relationship of Dispersoids Precipitated in an AA3XXX Alloy during Annealing at Low Temperatures. , 2012, , 1161-1166.		Ο
110	Synergetic effect of Er and Zr on the precipitation hardening of Al–Er–Zr alloy. Scripta Materialia, 2011, 65, 592-595.	2.6	177
111	X-Ray Videomicroscopy Studies of Eutectic Al-Si Solidification in Al-Si-Cu. Metallurgical and Materials Transactions A: Physical Metallurgy and Materials Science, 2011, 42, 170-180.	1.1	42
112	X-Ray Video Microscopy Studies of Irregular Eutectic Solidification Microstructures in Al–Si–Cu Alloys. ISIJ International, 2010, 50, 1936-1940.	0.6	2
113	Microstructure evolution of commercial pure titanium during equal channel angular pressing. Materials Science & Engineering A: Structural Materials: Properties, Microstructure and Processing, 2010, 527, 789-796.	2.6	80
114	Physicochemical characterisation of combustion particles from vehicle exhaust and residential wood smoke. Particle and Fibre Toxicology, 2006, 3, 1.	2.8	141
115	Ge nanoparticle formation and photoluminescence in Er doped SiO2 films: influence of sputter gas and annealing. Microelectronics Journal, 2005, 36, 531-535.	1.1	8
116	The 1.54-μm photoluminescence from an (Er, Ge) co-doped SiO[sub 2] film deposited on Si by rf magnetron sputtering. Applied Physics Letters, 2004, 85, 4475.	1.5	36
117	Solidification structures and phase selection of iron-bearing eutectic particles in a DC-cast AA5182 alloy. Acta Materialia, 2004, 52, 2673-2681.	3.8	51
118	Evolution of eutectic intermetallic particles in DC-cast AA3003 alloy during heating and homogenization. Materials Science & Engineering A: Structural Materials: Properties, Microstructure and Processing, 2003, 347, 130-135.	2.6	100
119	Quantitative study on the precipitation behavior of dispersoids in DC-cast AA3003 alloy during heating and homogenization. Acta Materialia, 2003, 51, 3415-3428.	3.8	255
120	Easy glass formation in magnesium-based Mg-Ni-Nd alloys. Journal of Materials Science, 1996, 31, 1857-1863.	1.7	28
121	Influence of Mg Content, Grain Size and Strain Rate on Mechanical Properties and DSA Behavior of Al-Mg Alloys Processed by ECAP and Annealing. Materials Science Forum, 0, 794-796, 870-875.	0.3	3
122	Microstructural Evolution during Isothermal Annealing of a Cold-Rolled Al-Mn-Fe-Si Alloy with Different Microchemistry States. Materials Science Forum, 0, 794-796, 1163-1168.	0.3	8
123	Orientation Studies of α-Al(Fe,Mn)Si Dispersoids in 3xxx Al Alloys. Materials Science Forum, 0, 794-796, 39-44.	0.3	7
124	Microstructure and properties of nano-C and in-situ Al2O3 reinforced aluminum matrix composites processed by high-pressure torsion. Composite Interfaces, 0, , 1-17.	1.3	2